Electron acceleration by an intense short-pulse laser in underdense plasma

M. Y. Yu, Wei Yu, Z. Y. Chen, J. Zhang, Y. Yin, L. H. Cao, P. X. Lu, and Z. Z. Xu

Citation: Physics of Plasmas (1994-present) **10**, 2468 (2003); doi: 10.1063/1.1572158
View online: http://dx.doi.org/10.1063/1.1572158
View Table of Contents: http://scitation.aip.org/content/aip/journal/pop/10/6?ver=pdfcov
Published by the AIP Publishing

Electron acceleration by an intense short-pulse laser in underdense plasma

M. Y. Yu
Institut für Theoretische Physik I, Ruhr-Universität Bochum, D-44780 Bochum, Germany

Wei Yu
Shanghai Institute of Optics and Fine Mechanics, Shanghai 201800, People's Republic of China

Z. Y. Chen
Institut für Theoretische Physik I, Ruhr-Universität Bochum, D-44780 Bochum, Germany and Department of Chemistry, University of Antwerp, B-2610 Wilrijk-Antwerp, Belgium

J. Zhang
Institute of Physics, Chinese Academy of Sciences, Beijing 100080, People's Republic of China

Y. Yin and L. H. Cao
National University of Defense Technology, Changsha 410073, People's Republic of China

P. X. Lu and Z. Z. Xu
Shanghai Institute of Optics and Fine Mechanics, Shanghai 201800, People's Republic of China

(Received 23 October 2002; accepted 10 March 2003)

Electron acceleration from the interaction of an intense short-pulse laser with low density plasma is considered. The relation between direct electron acceleration within the laser pulse and that in the wake is investigated analytically. The magnitude and location of the ponderomotive-force-caused charge separation field with respect to that of the pulse determine the relative effectiveness of the two acceleration mechanisms. It is shown that there is an optimum condition for acceleration in the wake. Electron acceleration within the pulse dominates as the pulse becomes sufficiently short, and the latter directly drives and even traps the electrons. The latter can reach ultrahigh energies and can be extracted by impinging the pulse on a solid target. © *2003 American Institute of Physics*. [DOI: 10.1063/1.1572158]

I. INTRODUCTION

Rapid advances in short-pulse high-intensity lasers have given rise to many new applications. There is thus much interest in the physics of the interaction of intense short-pulse lasers with plasmas and solids. Simulations and experiments have shown that very energetic electrons are produced when an intense short-pulse laser interacts with a low-density plasma or impinges on a solid target. High-energy electrons have many applications, such as in fast ignition of fusion reaction,[1,2] hard x-ray source,[3–5] fast ion production,[6–8] etc. Several theories for high-energy electron generation by laser light have been proposed. These include resonance absorption,[9] $\mathbf{v}\times\mathbf{B}$ heating,[10] vacuum heating,[11] nonadiabatic heating at the plasma–light interface,[12] and stochastic heating,[13] etc. In most of these theories the laser light interacts with the electrons at or near the target surface as a *standing* wave.

When an intense short laser pulse propagates in an underdense plasma, the electrons are accelerated and decelerated by the ponderomotive force at its leading and trailing halves, respectively. The spatial displacement of the electrons can give rise to a large space charge field, whose relaxation after the pulse moves away can lead to strong electrostatic wake oscillations.[14,15] A small number of electrons in the wake field can reach very high energies and they are released when wave breaking occurs. On the other hand, the ponderomotively accelerated electrons inside a sufficiently short laser pulse can also reach very high energies. These energetic electrons can be extracted (before they are decelerated) by letting the laser pulse hit a solid target.[16,17] Physically, electron acceleration inside a laser pulse and inside the laser-excited wake oscillation are separate but closely related processes. The latter are in fact governed by the same equations and can compete with each other. An understanding of the details of the relation between these processes would be helpful in the design of advanced schemes of wake and direct acceleration of electrons. However, they have traditionally been investigated separately. In this paper we investigate the interaction of a very short laser pulse with a plasma, such that the pulse width is less than the plasma-wave length, a situation that occurs in the very rarefied preplasma region of the interaction. In order to clarify the relationship between the two and their relative effectiveness under different conditions, we consider in a unified and transparent manner the electron dynamics in the wake and within the laser pulse. It is found and expressed quantitatively that the relative efficiencies of the two acceleration processes depend on the laser intensity and pulse width, as well as the background plasma density. The results are compared with that from a two-dimensional (2D) particle-in-cell (PIC) simulation.

II. GOVERNING EQUATIONS

When a short planar light pulse propagates in a uniform low-density plasma, the response of the plasma electrons can be described by[15,18]

$$\mathbf{v}_\perp = \mathbf{a}/\gamma, \tag{1}$$

$$\partial_t(\gamma v_z) = \partial_z(\phi - \gamma), \tag{2}$$

$$\partial_t n = -\partial_z(n v_z), \tag{3}$$

$$\partial_z^2 \phi = n - Z n_i, \tag{4}$$

where $\mathbf{v}$ is the electron velocity normalized by c, $\mathbf{A}$ and ϕ are the vector and scalar potentials normalized by mc^2/e, t is the time normalized by ω^{-1}, the space coordinates are normalized by k^{-1}, where ω and k are the laser frequency and wave number, respectively. Furthermore, $\gamma = (1-v^2)^{-1/2}$ is the relativistic factor or the normalized (by mc^2) electron energy, n and n_i are the electron and ion densities normalized by the critical density, and Z is the ion charge number. On the time scale of the light pulse and electron motion, the heavy ions are not much affected, so that n_i can be taken as a constant.

We assume that the plasma density is low, the laser intensity high, and the pulse width short, so that the normalized envelope $a = |\mathbf{A}|$ of the vector potential of the laser pulse can be taken to be nonevolving and that it propagates at a constant speed near that of light in the plasma.[15,19] Thus a is a function of $\xi = z - v_g t$, where $v_g = \sqrt{1 - Z n_i}$ is the constant group velocity of the light waves in the plasma. Integrating Eqs. (2) and (3) and using the boundary condition that the plasma is undisturbed and homogeneous before the laser pulse arrives, or $v_z = 0$, $\phi = 0$, and $n = Z n_i$ at $z = \infty$, one easily obtains the governing equations[15]

$$\phi - \gamma + \gamma v_z v_g = -1, \tag{5}$$

$$n(v_z - v_g) = -Z n_i v_g. \tag{6}$$

Eliminating n, v_z, and γ, one obtains from Eq. (4),

$$d_\xi^2 \phi = v_g(1+\phi)/\sqrt{(1+\phi)^2 - Z n_i(1+a^2)} - 1, \tag{7}$$

for ϕ. Equation (7) together with (5) and (6) govern the quasistationary dynamics of the electrons inside as well as behind the laser pulse. Weak transient behavior and damping of the light wave and wake oscillations are neglected. Equation (7) is highly nonlinear and inhomogeneous, but it can be easily integrated numerically.

III. HEURISTIC DESCRIPTION

It is instructive to first review and discuss qualitatively the interaction of a laser pulse with the plasma electrons under nonrelativistic conditions. As the pulse propagates in the plasma, the ponderomotive force at its rising front accelerates the electrons forward, creating a local charge separation, which tends to counteract the motion of the accelerating electrons. The electrons are also decelerated by the ponderomotive force exerted by the trailing part of the pulse. The strength and distribution of the charge separation field thus depend on the intensity, speed, and the width of the pulse, as well as the unperturbed electron density.

In general, the uncompensated electrostatic space charge field remains after the laser pulse passes. The relaxation of this field from electron redistribution then gives rise to the electron wake oscillations having a phase speed near the speed of the light pulse and a frequency near the plasma frequency. The normalized wavelength λ_p of the wake oscillations is approximately v_g/ω_p, or $2\pi/\sqrt{Z n_i}$, which is a function only of the plasma density. One expects that the efficiency of wake field generation is highest[14] if the separation between the ponderomotive acceleration and deceleration of the electrons by the laser pulse is half λ_p, so that the plasma wave and the ponderomotive force are locally phase matched or "resonant" in a region of about half a plasma wavelength.

On the other hand, if the laser pulse width is much smaller than the optimum value, the dynamics of the electrons therein can be so dominated by the ponderomotive force that the they bunch inside the pulse, at the expense of the downstream (in the pulse frame) electrons. In this case the electrons are trapped by the pulse. Wake oscillations can still be excited by the space charge field behind it. However, they will be much weaker than that of the optimum case.

IV. RESULTS

For the purpose of tracking the electron energy gain within the laser pulse, it is convenient to introduce the parameter

$$\eta = \left(\int a^2 d\xi \right)^{-1} \int 2n(\gamma - 1) d\xi, \tag{8}$$

where the integral is over the laser pulse. Thus, η is the ratio of the energy of the electrons inside the pulse to that of the laser. For a Gaussian pulse, a^2 is given by

$$a^2 = \tfrac{1}{2} a_0^2 \exp(-\xi^2/L^2)[1 + \cos(2\xi)], \tag{9}$$

for linearly polarized light, and

$$a^2 = a_0^2 \exp(-\xi^2/L^2), \tag{10}$$

for circularly polarized light, respectively. Here, $L = d/2$, and d is the pulse width. This difference in a^2 leads to a strong dependence of the results on the polarization, as will be discussed below. The response of the electrons to the laser pulse can be calculated numerically from Eqs. (5)–(7).

In the numerical evaluation, the electrostatic field and electron density are calculated in the presence of the given $a(\xi)$. The integration is initiated at a large positive ξ in front of the pulse where a is negligibly small. Both the electrostatic field and its derivative start from zero there. The integration is then carried out backwards, so that an overall picture of the electron dynamics and electric field behavior in the pulse and wake is obtained. We shall investigate both regions under the same laser and plasma conditions in order to determine the efficiencies of the two electron acceleration mechanisms.

A. Effectiveness of acceleration in the wake and in the pulse

In Fig. 1, the plasma response to a circularly polarized laser pulse is presented for $Z n_i = 10^{-4}$, and (a) $a_0 = 0.05$ and (b) $a_0 = 2$ and 5. The solid lines show the maximum wake field amplitude $\phi_{\max}/a_0$ (here renormalized for the convenience of comparing with the laser field) as a function of

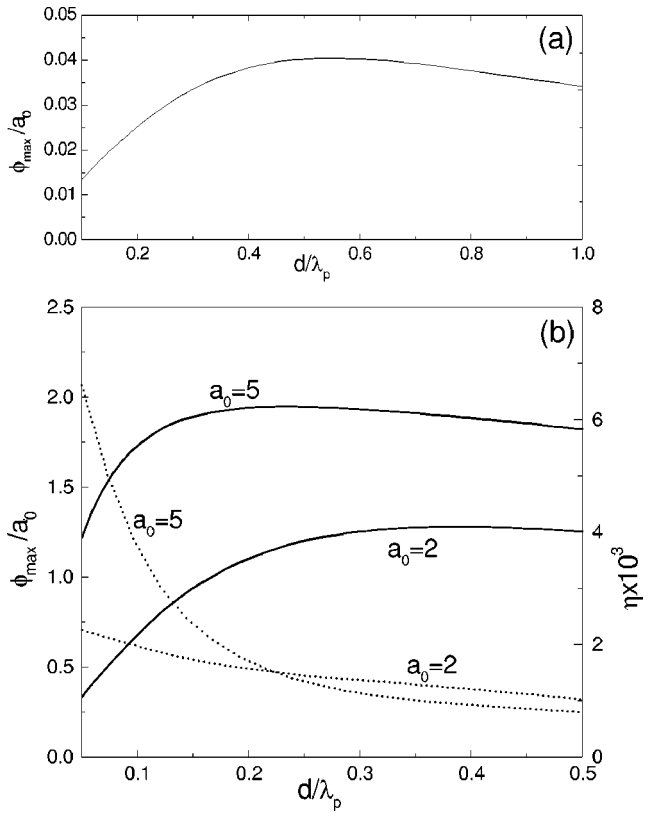

FIG. 1. Maximum wake amplitude (solid lines, renormalized by a_0) $\phi_{\max}/a_0$ as a function of d/λ_p for $Zn_i=10^{-4}$, with (a) $a_0=0.05$ and (b) $a_0=2$ and 5. The dependence of the energy ratio η on d/λ_p is given by the dotted lines in (b). For the parameters chosen η is rather small (it is even smaller for the $a_0=0.05$ case in (a) and is therefore not shown), which is consistent with our assumption of constant laser intensity and negligible ion motion.

d/λ_p. Figure 1(a) shows that in the nonrelativistic regime the optimum pulse width for wake generation is about half a plasma wavelength as expected.[14] In this case of relatively weak laser intensity, the laser pulse generates a charge separation field, which induces sinusoidal wake oscillations[14] typical of linear waves. Even for this case one can achieve a wake field amplitude of $\phi_{\max}/a_0 \sim 0.8$. The charge separation field and wake potential can be increased by increasing the laser intensity. However, to optimize the process it is necessary to shorten the laser pulse since the intensity of the ponderomotive force affects the charge separation field. Figure 1 also shows that $\phi_{\max}/a_0$ decreases rapidly (slowly) with d/λ_p if the laser pulse width goes below (above) its optimum value.

The dependence of the normalized electron energy η inside the pulse on the pulse width is given by the dotted lines in Fig. 1(b). It is too small to be shown clearly in Fig. 1(a), which is for small $a_0(=0.05)$. One can see that in general η increases with decreasing pulse width and increasing intensity of the laser. That is, for the same background plasma density, direct acceleration by the laser pulse is dominant for short and intense pulses.

B. Large amplitude wake oscillations

As the laser intensity increases, the optimum pulse width becomes smaller. Although the interaction scenario inside the laser pulse is physically similar to that of weaker pulses, a much stronger charge separation field is created. In fact, the wake oscillations can be of higher amplitude than that of the laser, or $\phi > a_0$, and they can become highly nonlinear. In Fig. 2, the laser–plasma interaction scenario and wake field generation process for a circularly polarized intense laser pulse is presented. Here, $a_0=2$ and $d=0.35\lambda_p$, corresponding to the optimum width for wake generation (see Fig. 1). The background electron density is again $Zn_i=10^{-4}$. The spatial behavior of the normalized vector and scalar potentials a and ϕ, the normalized longitudinal electron momentum $p_z=\gamma v_z$, and the renormalized electron density n/Zn_i are given by the dotted, dashed, solid, and dotted–dashed lines, respectively.

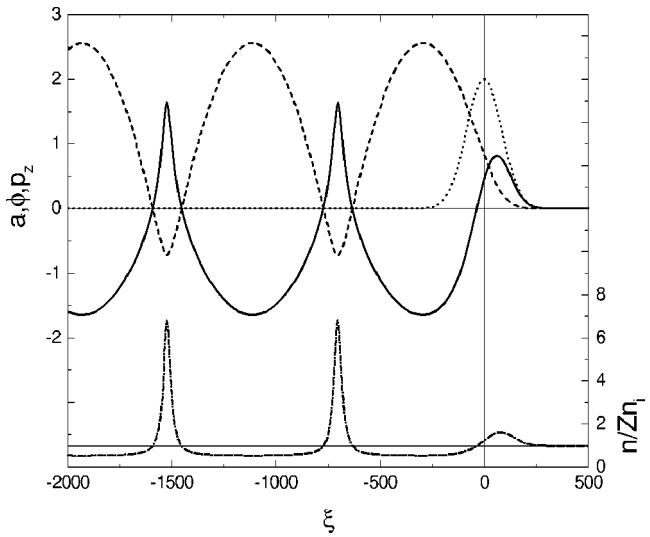

FIG. 2. Evolution of the normalized vector (a, dotted line) and scalar (ϕ, dashed line) potentials, longitudinal electron momentum (p_z, solid line), and electron density (n/Zn_i, dotted–dashed line), for $a_0=2$ and $Zn_i=10^{-4}$. Here, $d=0.35\lambda_p$, corresponding to the optimum width for wake generation.

Inside the laser pulse, the electrons are accelerated and decelerated by the ponderomotive forces arising from the high gradients at the front and back of the laser envelope. Their displacement leads to a strong charge separation field, which in turn tends to restrict the motion of the displaced electrons as well as to induce motion by the neighboring electrons. After the pulse passes a large space charge field remains and its relaxation leads to highly nonlinear wake plasma oscillations. The electron density profile in the latter is characterized by localized peaks separated by shallow and flat depressions, characteristic of nonlinear plasma oscillations[21,22] even in the absence of relativistic effects. It is of interest to point out that, except for the larger amplitudes of the physical quantities involved and the highly nonlinear wake oscillation, the scenario of the laser–plasma interaction in this case is still very similar to the low intensity case.

C. Direct electron acceleration in the laser pulse

Figure 3 is also for a circularly polarized laser with $a_0=2$, but much narrower pulse width ($d=0.05\lambda_p$). The latter

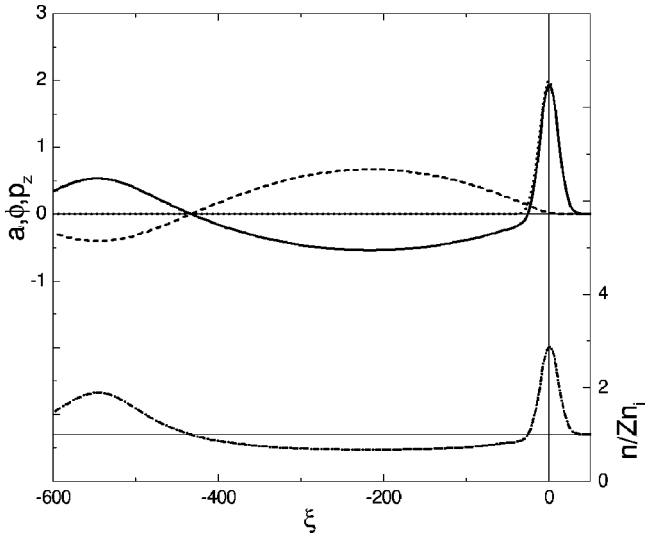

FIG. 3. Same as Fig. 2, but for a much shorter pulse width ($d=0.05\lambda_p$) than that of optimum for wake generation.

is much less than the width $\sim 0.35\lambda_p$ [see Fig. 1(b)] for optimum wake excitation. This case differs considerably from that of Fig. 2, and corresponds to direct electron acceleration by the laser pulse. Here a significant change (with respect to that of Fig. 2) in the behavior of the electron dynamics within the laser pulse occurs: the electron momentum and density profiles become nearly synchronized with that of the laser pulse. The electrons are strongly accelerated and decelerated by the predominating ponderomotive force at the leading and trailing fronts of the pulse, respectively.

In this case, the laser pulse traps the electrons and carries them with it as a soliton-like system, such as that found by Kaw *et al.*[23] The space charge field created by the electron bunching within the pulse is entirely downstream. Furthermore, this space charge field is weaker, and the number density and energy involved in the wake oscillations less, than that inside the laser pulse. They are also less than that for longer pulses (such as that in Fig. 2). It is of interest to note that this wake field reduction also occurs for weak laser intensities if the pulse is sufficiently short, since besides the lack of the local phase-matching between the ponderomotive force induced space charge field and the wake oscillations, the number of ponderomotively displaced electrons, and thus also the space charge field, is much less. The intermediate cases (not shown) shows that the transition from wake to direct acceleration when the pulse width becomes less than that of the optimum is rapid but continuous, as is also indicated in Fig. 1(b). In the latter figure one can also see that for the high intensity ($a_0=5$) case η increases rapidly as the pulse width is decreased, despite the fact that the number of electrons that can be accelerated in a short pulse is small.

D. Effect of background density

Besides the intensity a_0 and width d of the laser pulse, another important factor governing the behavior of the laser–plasma interaction is the density of the background electrons available for acceleration. In Figs. 4(a) and 4(b), the maximum electron energy and density of the ponderomotively bunched electrons are shown as functions of the laser strength a_0 for $d=5$, and $Zn_i=10^{-4}$ (solid curve, corresponding to $d/\lambda_p=0.05$). Recall that $\lambda_p=2\pi/\sqrt{Zn_i}$ and all lengths are normalized by the laser wavelength. and $Zn_i=10^{-3}$ (dotted curve, corresponding to $d/\lambda_p=0.16$), respectively. One can see that in both cases the maximum energy and density increase with the laser strength, as was already discussed. Figure 4 also shows that in plasmas of lower density the electrons bunched and accelerated by the laser pulse will have higher energy but lower density.

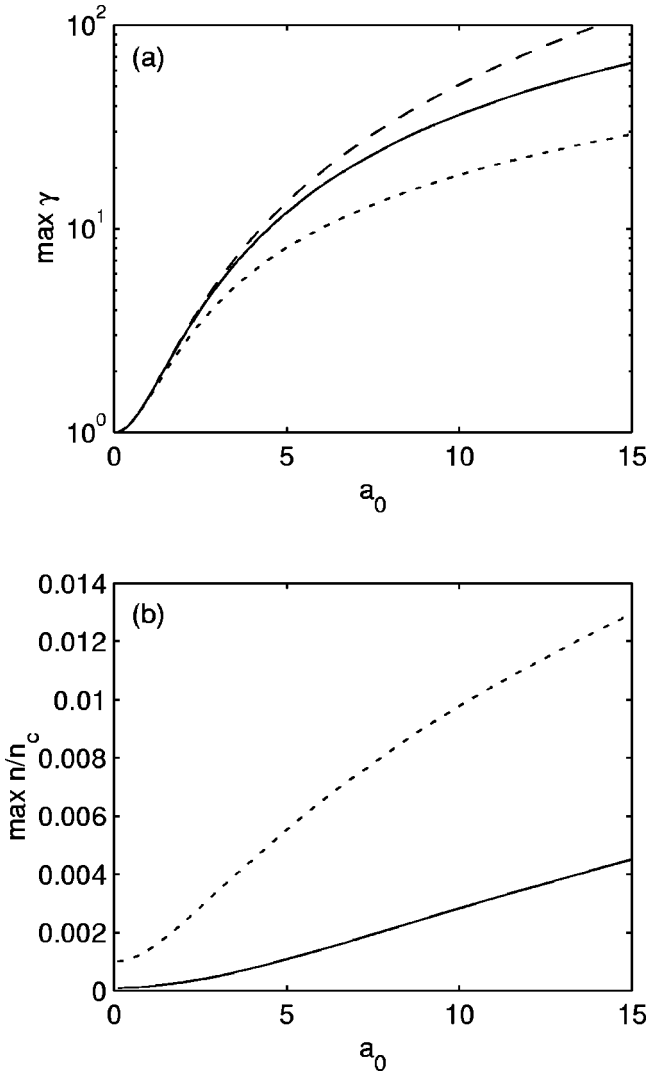

FIG. 4. Maximum electron energy γ (a) and density n/n_c (b) of the ponderomotively bunched electrons in the laser pulse vs the laser strength a_0, for $d=5\lambda$, and $Zn_i=10^{-4}$ (solid curve) and $Zn_i=10^{-3}$ (dotted curve), respectively. The dashed curve in (a) is for $Zn_i=0$ or $v_g=1$.

For completeness, the dashed curve in Fig. 4(a) shows the maximum electron energy for the case $Zn_i=0$ (no background ions). Here $v_g=1$ and $\phi=0$, and the problem reduces to the ponderomotive acceleration of an electron by a laser pulse propagating in vacuum. We then get from Eq. (1) and the definition of γ the well-known scaling,

$$\gamma_{\max}-1=a_0^2/2, \tag{11}$$

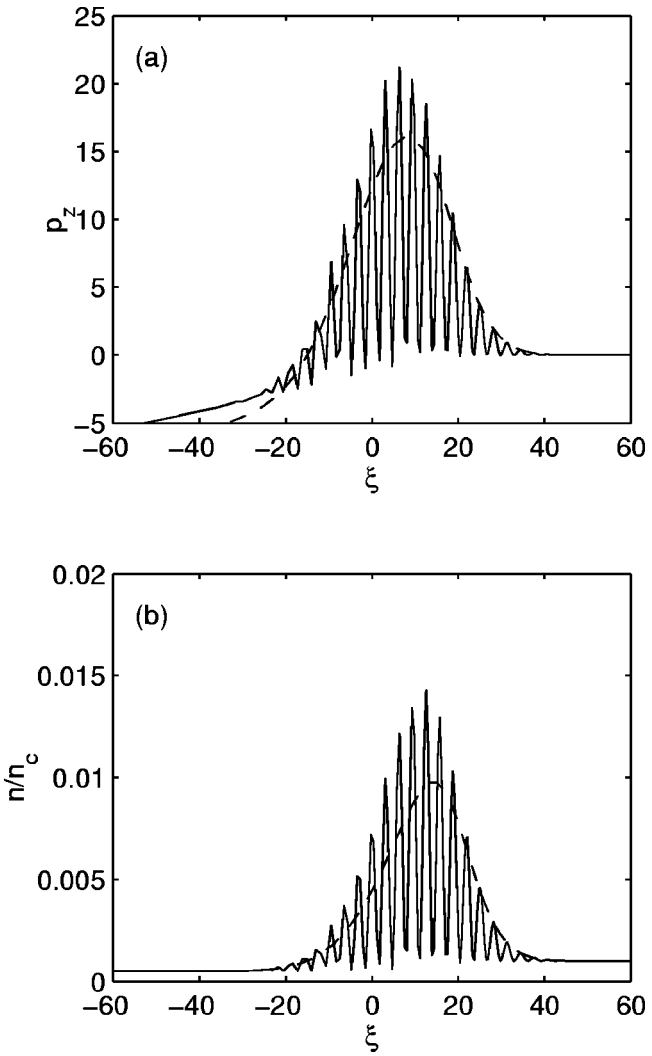

FIG. 5. Longitudinal electron momentum (a) and density (b) for linear (solid curve) and circular (dashed curve) polarizations, for $Zn_i=10^{-3}$, $a_0=10$, and $d=5\lambda$. The pulse width is again much smaller than that of optimum.

which shows that the electron acceleration and bunching processes discussed here are simply the relativistic ponderomotive acceleration of electrons *in a plasma*. In this case a self-consistent charge separation field appears when the electrons are displaced from the stationary ions.

E. Effect of polarization

Up to now we have concentrated on circularly polarized laser light. Figure 5 shows the effect of polarization. For both linear (solid curve) and circular (dashed curve) polarizations, the profiles of the longitudinal electron momentum and density are shown for $Zn_i=10^{-3}$, $a_0=10$, and $d=5\lambda$. The pulse width is again much smaller than half a plasma wavelength ($\sim 16\lambda$). The density and momentum profiles for the linear polarization case exhibit oscillatory behavior, which is due to the $\cos(2\xi)$ term in Eq. (9). Such a longitudinal modulation at twice the laser frequency appears only for linearly polarized light. It is from the oscillating component (which

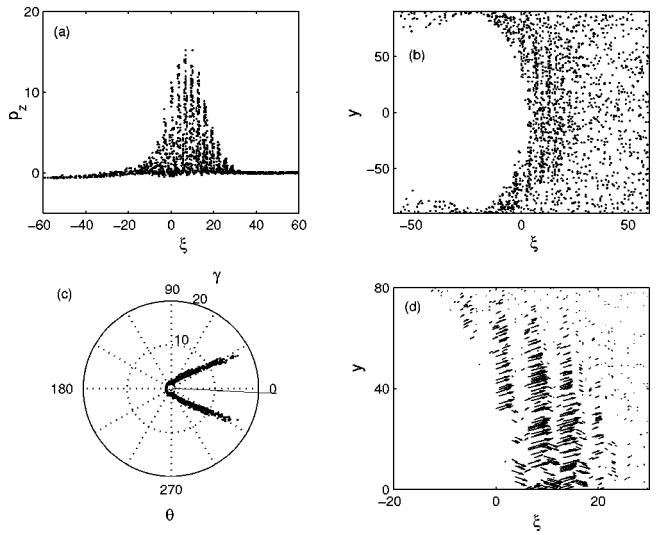

FIG. 6. Results from 2D PIC simulations of a tightly focused linearly polarized pulse in a rarefied plasma. The parameters are the same as in Fig. 5. (a) Longitudinal electron momentum vs the axial coordinate. (b) 2D spatial distribution of the electron density. (c) Angular distribution of the electron energy. The concentric circles from the center represent $\gamma=1$,10, and 20, respectively. (d) Distribution of the electron momentum vectors.

does not appear for circularly polarized light) of the ponderomotive force, similar to that appearing in the well-known $\mathbf{u}\times\mathbf{B}$ heating effect.[10]

F. Higher dimensional effects

So far we have investigated electron acceleration in the propagation direction of an intense short-pulse laser using a one-dimensional (1D) analysis. Although it can be expected that the 1D approach is sufficient for the highly directional processes considered,[14] in order to verify our results we have also carried out a 2D PIC simulation of a narrowly focused laser pulse in a low density plasma. In the simulation the laser pulse is assumed to have a narrow Gaussian profile in the transverse direction. The results are given in Fig. 6. In order to show the distributions more clearly, only 1/5 of the simulated electrons is represented in the figures. Figure 6(a) and (b) show the axial momentum and density distributions of the electrons in a linearly polarized laser pulse. The parameter values are the same as in Fig. 5. We see that the longitudinal electron momentum Fig. 6(a) is in good agreement with that of Fig. 5(a) obtained from the 1D analytical theory. Figure 6(b) shows that electrons are accelerated forward and a vacuum region or hole is formed in the tail of the laser pulse since now there is also a transverse ponderomotive force. As a result, the wake oscillation (not shown) appears as a series of electron holes. In the enhanced density region at the center, one can also see the local compression patterns formed by the *periodic* ponderomotive force of the linearly polarized light pulse. The angular dependence of the electron energy γ is shown in Fig. 6(c). The transverse spread is due to the ponderomotive force arising from the transverse profile of the laser pulse. If the laser were not so tightly focused, the transverse electron motion would be governed mainly by the laser field, as given by Eq. (1). In this

case the electrons would be (net) accelerated only in the axial direction. Figure 6(d) gives (in an enlarged region) the spatial distribution of the electron momentum vectors. One can again see the oscillatory nature of the longitudinal ponderomotive force. Electron acceleration is mainly in the forward direction and it occurs at the center of the pulse. Thus, together with the results from existing experiments[17] and 2D numerical calculations,[25] as well as other simulations,[16] our simulation shows that for *longitudinal electron acceleration* in the pulse and the wake, despite the significant difference in the actual configurations, 1D analyses yield quite accurate conclusions.

V. DISCUSSION

Using a simple one-dimensional analytical model, we have in this paper considered the relation between direct acceleration of electrons in a short intense laser pulse and acceleration in the laser-excited wake field. The two processes can compete with each other. Their relative importance depends on the response of the electrons to the pulse and is governed by the laser intensity and pulse width, as well as the background plasma density. For longer pulse lasers, especially when local phase matching in the laser pulse between the ponderomotive force and the wake plasma oscillation occurs, there is strong electron acceleration in the laser-excited wake field and little acceleration or trapping inside the laser pulse. For sufficiently short and intense pulses, there is strong acceleration of the electrons inside the pulse, and the corresponding wake field acceleration becomes much weaker. Direct acceleration of electrons inside the laser pulse is no other than the ponderomotive acceleration of electrons in a plasma by the laser pulse. Its effectiveness depends on the number of background electrons available and therefore the unperturbed plasma density. In low density plasmas the ponderomotively accelerated electrons will have higher energy but lower density. Furthermore, for linearly polarized lasers the ponderomotively bunched electrons inside the pulse exhibit longitudinal oscillation at twice the laser frequency because of the oscillating component of the ponderomotive force.

Depletion of the laser energy has not been included in our theory. For higher background plasma densities, the reaction of the electron motion on the propagation of the laser pulse should be considered.[18,23,25] For long ($\gg 1$ ps) pulses, higher dimensional and ion effects can also enter. However, investigations of related problems[19,23,24] including self-consistent laser intensities and/or ion effects seem to indicate that these effects do not significantly change the one-dimensional electron energization behavior in the laser–plasma interaction process under consideration here.

It is of interest to mention that in their study of short-pulse laser propagation in highdensity ($N_e \sim 10^{20}$ cm^{-3}, corresponding to $Zn_i \sim 0.1$ under the conditions of the present work) plasmas, Feit *et al.*[2] found that the laser–plasma interaction is unstable for short-wavelength longitudinal perturbations. However in that regime, $(N_e/N_c)^{1/2}$ is not small, and $L_p > k_p^{-1}$ (or $d > \lambda_p$) always holds. On the other hand, in the regime considered here the opposite condition $L_p < k_p^{-1}$ (or $d < \lambda_p$) holds. That is, we confine ourselves to low-density plasmas with $Zn_i = 10^{-4} - 10^{-3}$, corresponding to the very low-density preplasma region that is normally produced by a much weaker prepulse or the low-intensity leading front of a high-intense laser pulse in laser–matter interactions. It should be emphasized that only at such low plasma densities the laser pulse width can be smaller than the plasma wavelength.

In practical applications, the highest-energy electrons in the large amplitude wake oscillation will be released when wave breaking occurs at the wave peaks.[14,20] They can also be enhanced and extracted by elaborate methods. On the other hand, the ponderomotively accelerated ultrahigh energy electrons in the rising front of the pulse can be easily extracted by impinging the laser pulse onto a solid target.[16,17] The pulse will then be reflected and the high energy electrons released into the target without suffering the ponderomotive deceleration in the trailing part of the pulse. The parameter η may then be considered as a coefficient of laser light absorption by the trapped (and released) electrons. Furthermore, the reflected pulse can also interact with the wake and significantly modifying the wake oscillation, leading to additional acceleration and the option of producing backward propagating ultrahigh energy electrons.[5,16]

ACKNOWLEDGMENTS

This work was supported by the Max Planck Society–Chinese Academy of Sciences Exchange Program, the National High-Technology Program of China (Contract No. 863-416-1), and the National Natural Sciences Foundation of China (Contract No. 19974058).

[1] M. Tabak, J. Hammer, M. E. Glinsky, W. L. Kruer, S. C. Wilks, J. Woodworth, E. M. Campbell, M. D. Perry, and R. J. Mason, Phys. Plasmas **1**, 1626 (1994).
[2] M. D. Feit, J. C. Garrison, and A. M. Rubenchik, Phys. Rev. E **53**, 1068 (1996).
[3] P. A. Norreys, M. Santala, E. Clark *et al.*, Phys. Plasmas **6**, 2150 (1999).
[4] Y. Sentoku, K. Mima, T. Taguchi, S. Miyamoto, and Y. Kishimoto, Phys. Plasmas **5**, 4366 (1998).
[5] R. Kodama, K. A. Tanaka, Y. Sentoku, T. Matsushita, K. Takahashi, H. Fujita, Y. Kitagawa, Y. Kato, T. Yamanaka, and K. Mima, Phys. Rev. Lett. **84**, 674 (2000).
[6] T. Zh. Esirkepov, Y. Sentoku, K. Mima *et al.*, JETP Lett. **70**, 82 (1999).
[7] G. S. Sarkisov, V. Yu. Bychenkov, V. N. Novikov, V. T. Tikhonchuk, A. Maksimchuk, S.-Y. Chen, R. Wagner, G. Mourou, and D. Umstadter, Phys. Rev. E **59**, 7042 (1999).
[8] M. Hegelich, S. Karsch, G. Pretzler *et al.*, Phys. Rev. Lett. **89**, 085002 (2002).
[9] N. A. Ebrahim, H. A. Baldis, C. Joshi, and R. Benesch, Phys. Rev. Lett. **45**, 1179 (1980).
[10] W. L. Kruer and K. Estabrook, Phys. Fluids **28**, 430 (1985).
[11] F. Brunel, Phys. Rev. Lett. **59**, 52 (1987).
[12] S. C. Wilks, W. L. Kruer, M. Tabak, and A. B. Langdon, Phys. Rev. Lett. **69**, 1383 (1992).
[13] J. M. Rax, Phys. Fluids B **4**, 3962 (1992).
[14] T. Tajima and J. M. Dawson, Phys. Rev. Lett. **43**, 267 (1979).
[15] E. Esarey, P. Sprangle, J. Krall, and A. Ting, IEEE Trans. Plasma Sci. **24**, 252 (1996).
[16] W. Yu, V. Bychenkov, Y. Sentoku, M. Y. Yu, Z. M. Sheng, and K. Mima, Phys. Rev. Lett. **85**, 570 (2000).
[17] R. A. Snavely, M. H. Key, S. P. Hatchett *et al.*, Phys. Rev. Lett. **85**, 2945 (2000).

[18]M. Y. Yu, P. K. Shukla, and K. H. Spatschek, Phys. Rev. A **18**, 1591 (1978).
[19]P. Sprangle, E. Esarey, and A. Ting, Phys. Rev. Lett. **64**, 2011 (1990).
[20]J. F. Drake, Y. C. Lee, K. Nishikawa, and N. L. Tsintsadze, Phys. Rev. Lett. **36**, 196 (1976).
[21]J. M. Dawson, Phys. Rev. **113**, 383 (1959).
[22]R. C. Davidson, *Methods in Nonlinear Plasma Theory* (Academic, New York, 1972), Chap. 3.
[23]P. K. Kaw, A. Sen, and T. Katsouleas, Phys. Rev. Lett. **68**, 3172 (1992).
[24]F. Amiranoff, S. Baton, D. Bernard *et al.*, Phys. Rev. Lett. **81**, 995 (1998).
[25]S. V. Bulanov, V. A. Vshivkov, G. I. Dudnikova, T. Zh. Esirkepov, F. Califano, F. F. Kamenets, T. V. Liseikina, N. M. Naumova, and F. Pegoraro, Plasma Phys. Rep. **25**, 701 (1999).